International Conference on Control, Engineering & Information Technology (CEIT'13)
Proceedings Engineering & Technology - Vol.2, pp. 27-32, 2013

FOC Drive Scheme for a Photovoltaic Water PMSM-Pumping System

Samah Hammadi[1] Noureddine Hidouri[2] and Lassâad Sbita[3]

[1]hammadisamah@yahoo.fr, [2]noureddine.hidouri@yahoo.fr,[2]lassaad.sbita@enig.rnu.tn

Research Unit of Photovoltaic, Wind turbine and Geothermal Systems

National Engineering School of Gabes, Tunisia

***Abstract*— In this paper, the authors present a FOC drive scheme for an isolated photovoltaic water pumping system. The photovoltaic panel is used for supplying a centrifugal PMSM coupled pump. The permanent magnet synchronous motor (PMSM) receives the required active power from the photovoltaic panel (PV) through a buck converter and an inverter. The models of the photovoltaic panel, the PMSM, the buck converter, the inverter and the centrifuge pump are developed and used in the control scheme. The dynamic performances of the photovoltaic panel, the buck converter and the motor are analyzed. The simulation results have shown that the proposed methodology is an efficient solution of a fully control system.**

***Keywords*— Photovoltaic panel, water pumping system, FOC, PMSM, Buck converter.**

I. Introduction

In the remote areas as the mountains, the islands and the rural zones, where the electrification is a very delicate and expensive operation, the use of the renewable energy such as photovoltaic and wind energy is an improved solution for such applications as water pumping system [1-6].

Different types of motors are used for the water pumping system application such as DC motors [7], [8], Induction motors and permanent synchronous motors [3], [9].

Many techniques of control have been applied to permanent magnet synchronous as direct torque control (DTC) and field oriented control. The concept of field oriented control (FOC) is firstly developed by Blasche, [10]. The FOC is a flux-torque decoupling technique applied to AC machines. Two approaches are possible: the direct field orientation (DFO) based on the rotor flux angle given by a flux observer or estimator and the indirect field orientation (IFO) based on the rotor slip calculation, [11], [12].

In this paper a field oriented control is synthesized for permanent synchronous motor (PMSM) associated to an isolated photovoltaic water pumping system.

II. The Photovoltaic Water Pumping System Model

Fig. 1 shows the proposed photovoltaic water pumping system considered in this research work. The considered load is composed of a permanent synchronous motor (PMSM) coupled to a centrifuge pump, the motor receives the required voltage thought an inverter. In order to adapt the panel produced supply to the inverter need voltage, a buck converter is used. A storage battery is associated to storage the energy that can be used when the insulation is insufficient.

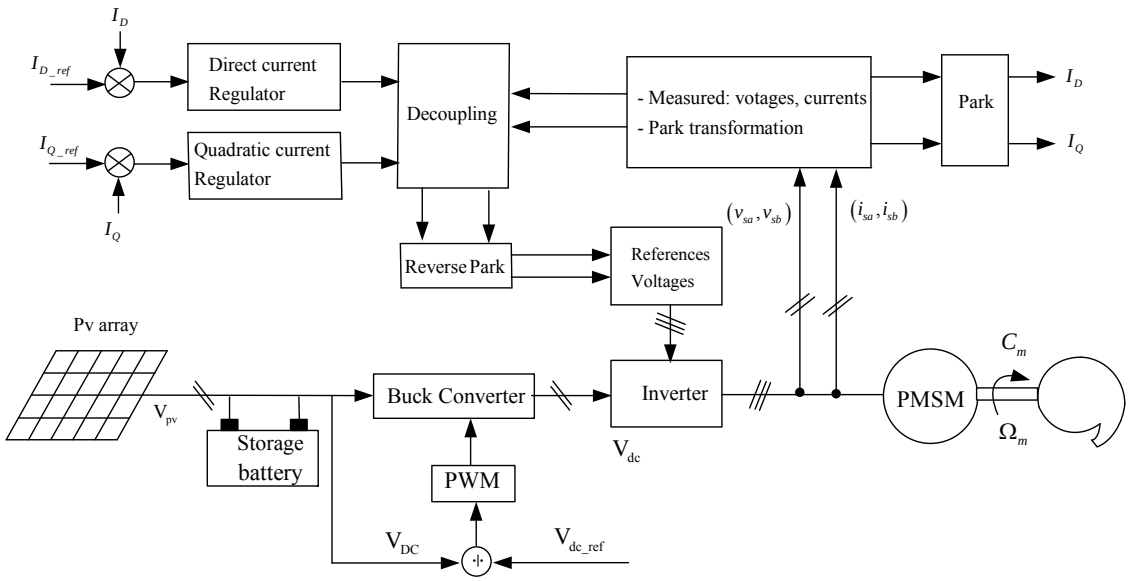

Fig. 1 Proposed wind turbine pumping system

A. Cell and PV Models

Photovoltaic cell is an electric component generally used to convert the solar energy to electrical energy. In the literature different model are used, [3], [13-17].

Denote by I_{ph} , D , R_{sc} and R_{pc} respectively the light-generated current source, the diode, the series and parallel resistances; the electric model used is this work is shown in fig. 2.

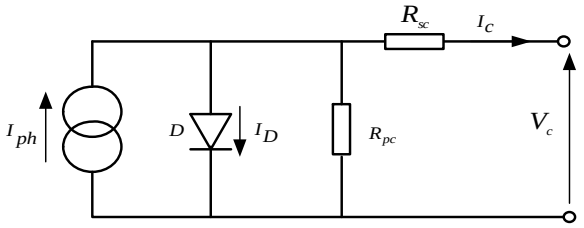

Fig. 2 Equivalent solar cell's electric circuit

At the reference condition characterized by the cell junction temperature T_{c_ref} and the insulation G_{ref} , the photocurrent I_{ph_ref} is equal to the reverse saturation current I_{sc_ref} .

The cell photocurrent I_{ph} is given by (1) where K_{SCT} represents the short circuit current temperature coefficient:

$$I_{ph} = \left[I_{sc\_ref} + K_{SCT} \left(T_c - T_{c\_ref} \right) \right] \frac{G}{G_{ref}} \tag{1}$$

The desired reverse saturation current I_{rs} can be expressed according to relation (2), where E_g , q , k and β are given in table II.

$$I_{rs} = I_{rs\_ref} \left(\frac{T_c}{T_{c\_ref}} \right)^3 \exp\left[\frac{qE_g}{\beta k} \left(\frac{1}{T_c} - \frac{1}{T_{c\_ref}} \right) \right] \tag{2}$$

The fundamental cell's characteristic is described by relation (3) relating the current I_c to the voltage V_c .

$$I_c = I_{ph} - \frac{\left(V_c + R_{sc} I_c \right)}{R_{pc}} - I_{rs} \left(\exp\left(\frac{q}{\beta k T_c} \left(V_c + R_{sc} I_c \right) \right) - 1 \right) \tag{3}$$

If we consider that the solar panel is composed of N_p branch of modules assembled in parallel configuration; each one formed of N_s modules assembled in series arrangement. Also, we consider that a module contain n_s cells associated in series configuration. Theses considerations express the relations between the panel's and the cells parameters as shown in relation (4).

$$\begin{cases} I_p = N_p I_c ; \; V_p = n_s N_s V_c \\ R_{sp} = \dfrac{n_s N_s}{N_p} R_{sc} \; ; R_{pp} = \dfrac{n_s N_s}{N_p} R_{pc} \end{cases} \tag{4}$$

In this consideration, the non-linear characteristic equation related the panel current I_p to its voltage V_p is shown in (5).

$$\begin{aligned} I_p = {} & \frac{N_p R_{pc}}{R_{sc} + R_{pc}} \left[I_{ph} - \frac{1}{n_s N_s R_{pc}} V_p \right] \\ & - \frac{N_p R_{pc}}{R_{sc} + R_{pc}} I_{rs} \left[\exp \frac{q}{\beta k T_c} \left(\frac{V_p}{n_s N_s} + \frac{R_{sc} I_P}{N_p} \right) - 1 \right] \end{aligned} \tag{5}$$

B. PMSM model

In the Concordia stationary reference frame, applied to the machine winding, the ohm's law is given by equation (6):

$$\bar{v}_s = R_s \, \bar{i}_s + \frac{d\bar{\varphi}_s}{dt} \tag{6}$$

The stator flux vector $\bar{\varphi}_s$ is linked to the stator current $\bar{i}_s$, the rotor flux $\bar{\varphi}_r$ and the electric rotor position θ_r by relation (7) :

$$\bar{\varphi}_s = \bar{\varphi}_r + \frac{L_q}{2} \left(\bar{i}_s - \bar{i}_s^* e^{2j\theta_r} \right) + \frac{L_d}{2} \left(\bar{i}_s + \bar{i}_s^* e^{2j\theta_r} \right) \tag{7}$$

The magnitude Φ_r of the rotor flux vector $\bar{\varphi}_r$ is constant so that we have at any instant:

$$\bar{\varphi}_r = \Phi_r e^{j\theta_r} \tag{8}$$

The electromagnetic torque is given by (9) where p is the pair pole number of the machine.

$$C_{em} = p \; \bar{\varphi}_s \wedge \bar{i}_s \tag{9}$$

Developing (9) leads to:

$$C_{em} = p(\varphi_{sd} \, i_{sq} - \varphi_{sq} \, i_{sd}) \tag{10}$$

When Park synchronous reference frame with the rotor is used, (6) becomes as follows, where ω_r is the electric rotor speed:

$$\bar{V}_s = R_s \, \bar{I}_s + j\omega_r \, \bar{\Phi}_s + \frac{d\bar{\Phi}_s}{dt} \tag{11}$$

The components of stator flux vector are linked to those of current vector by:

$$\Phi_{sd} = \Phi_r + L_d I_{sd} \quad (12)$$

$$\Phi_{sq} = L_q I_{sq} \quad (13)$$

C. Centrifugal pump model

The centrifugal pump model can be described by the will known mechanical characteristic illustrated in relation (14).

$$h = a_0\omega_r^2 - a_1\omega_r Q - a_2 Q^2 \quad (14)$$

The hydraulic power P_H and the load torque of the centrifugal pump can be described respectively by (15) and (16).

$$P_H = \rho g Q H \quad (15)$$

$$C_r = k_r \Omega^2 + C_s \quad (16)$$

The mechanical model of the electric motor can be described by (17) where f_m and C_r represent respectively the motor's friction coefficient and the hydraulic load torque of the centrifugal pump.

$$C_{em} = J_m \frac{d\Omega_m}{dt} + f_m \Omega_m + C_r \quad (17)$$

D. Buck Converter Model

The schematic of the buck converter power stage that provides a stepped-down voltage to the load is given in fig. 3, [3], [5].

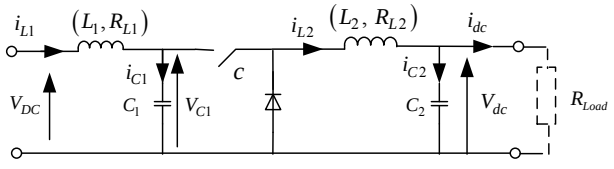

Fig. 3 Structure of the buck converter

We designate by c a Boolean variable that takes the value $(c=0)$ if the key is switched off and the diode is switched on and takes the value $(c=1)$ if the key is switched on and the diode is switched off. Thus, the model is given as, [5]:

$$\begin{bmatrix} \dot{i}_{L1} \\ \dot{i}_{L2} \\ \dot{V}_{c1} \\ \dot{V}_{c2} \end{bmatrix} = \begin{bmatrix} -\frac{R_{L1}}{L_1} & 0 & -\frac{1}{L_1} & 0 \\ 0 & -\frac{R_{L2}}{L_2} & \frac{c}{L_2} & -\frac{1}{L_2} \\ \frac{1}{C_1} & -\frac{c}{C_1} & 0 & 0 \\ 0 & \frac{1}{C_2} & 0 & -\frac{1}{R_{Load}C_2} \end{bmatrix} \begin{bmatrix} i_{L1} \\ i_{L2} \\ V_{C1} \\ V_{C2} \end{bmatrix} + \begin{bmatrix} \frac{1}{L_1} \\ 0 \\ 0 \\ 0 \end{bmatrix} V_{DC} \quad (18)$$

$$V_{out} = \begin{bmatrix} 0 & 0 & 0 & 1 \end{bmatrix} \begin{bmatrix} i_{L1} & i_{L2} & V_{C1} & V_{C2} \end{bmatrix}^t \quad (19)$$

E. Current and voltage inverter models

Fig. 4 shows the general diagram of a three-phase voltage inverter where the model including a geometric progression is presented in [3], [5].

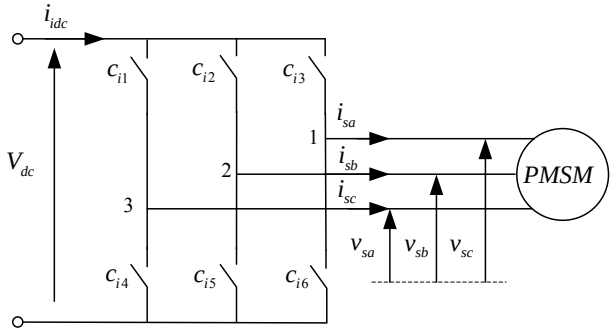

Fig. 4 Inverter-PMSM Configuration

In a fixed Concordia reference frame, the input inverter current i_{idc} can be derived from the PMSM stator current $\overline{i}_s$ and an inverter modulate function $\overline{s}_{ik}$ depending on the inverter keys states and expressed by the following relation where $(.)$ represent the scalar product:

$$i_{idc} = \sqrt{\frac{2}{3}} \overline{i}_s . \overline{s}_{ik} \quad (20)$$

The output inverter voltage is related to the input voltage by the following relation:

$$\overline{v}_s = \sqrt{\frac{2}{3}} V_{dc} \overline{s}_{ik} \quad (21)$$

The inverter modulate function $\overline{s}_{ik}$, defined and developed in the previous works [3], [5] and called inverter keys state vectors, is supported by 8 vectors that can be classified in two groups; the first one is composed of two null vectors, the second is composed of 6 active vectors that can be presented as a geometric progression defined by the first term 1 and the ratio $e^{j\frac{\pi}{3}}$, relation (22):

$$\begin{cases} \overline{s}_{ik} = 0 & if \quad k = 0 \quad or \quad k = 7 \\ \begin{cases} \overline{s}_{ik} = q^{(k-1)} \overline{s}_{i1} \\ \overline{s}_{i1} = 1 \\ q = e^{j\frac{\pi}{3}} \end{cases} & if \quad k = 1, 2, ...6 \end{cases} \quad (22)$$

The space representation of these vectors indicating the combination of the associated keys states (c_{i4}, c_{i5} *and* c_{i6}) is illustrated by fig. 5.

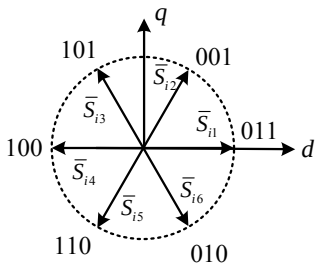

Fig.5 Diagram of the three-phase inverter state vectors

III. THE PMSM FIELD-ORIENTED CONTROL STRATEGY

After arrangement, the system of equation (11) can be represented by (23) where the different related terms are given by (24) and (25).

$$\begin{cases} V_{sd} = V_{sd1} - E_d \\ V_{sq} = V_{sq1} - E_q \end{cases} \tag{23}$$

$$\begin{cases} V_{sd1} = L_d \dfrac{dI_{sd}}{dt} + R_s I_{sd} \\ V_{sq1} = L_q \dfrac{dI_{sq}}{dt} + R_s I_{sq} \end{cases} \tag{24}$$

$$\begin{cases} E_d = \omega_r L_q I_q \\ E_q = -\left(\omega_r L_d I_d + \omega_r \Phi_r\right) \end{cases} \tag{25}$$

The direct and the quadratic transfer functions current/voltage are respectively given by (26) and (27).

$$\begin{cases} H_{Id}(p) = \dfrac{I_{sd}}{V_{sd1}} = \dfrac{K_d}{1+\tau_d p} \\ K_d = \dfrac{1}{R_s}\ ; \qquad \tau_d = \dfrac{L_d}{R_s} \end{cases} \tag{26}$$

$$\begin{cases} H_{Iq}(p) = \dfrac{I_{sq}}{V_{sq1}} = \dfrac{K_q}{1+\tau_q p} \\ K_q = \dfrac{1}{R_s}\ ; \qquad \tau_q = \dfrac{L_q}{R_s} \end{cases} \tag{27}$$

If the pole-zero cancellation method is used, the expressions and the parameters of the PI current controller can be respectively expressed by (28) and (29).

$$\begin{cases} C_{Id}(p) = K_{Id}\left(1 + \dfrac{1}{\tau_{Id} p}\right) \\ C_{Iq}(p) = K_{Iq}\left(1 + \dfrac{1}{\tau_{Iq} p}\right) \end{cases} \tag{28}$$

$$\begin{cases} K_{Id} = \dfrac{1}{K_d} = R_s\ ; \qquad \tau_{Id} = \tau_d = \dfrac{L_d}{R_s} \\ K_{Iq} = \dfrac{1}{K_q} = R_s\ ; \qquad \tau_{Iq} = \tau_q = \dfrac{L_q}{R_s} \end{cases} \tag{29}$$

IV. SIMULATION RESULTS AND DISCUSSION

The simulation in this work has been developed in Matlab/Simulink environment.

A. Analyses of physical sizes relating to the photovoltaic panel and the buck converter

The command of the buck converter is based on the DC voltage required by the load. This value is computed as a reference buck voltage term. The figures 6 and 7 give respectively the panel voltage and the output buck converter voltages. The second one (fig. 7) converges towards the required DC voltage according to the first one.

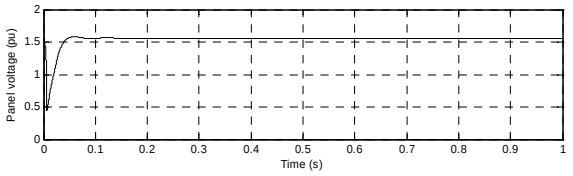

Fig. 6 Panel voltage response

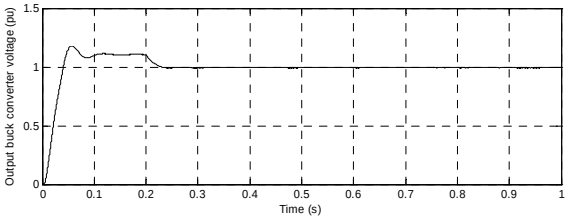

Fig. 7 Output buck converter voltage

In consideration of the rated motor current as a base value, fig. 8, fig. 9 and fig. 10 respectively give the panel current, the capacitance C1 current and the inductance L2 current. These figures show that the panel current is smoothly continuous with a good choice of the capacitance value relatively to that of the inductance. The alternative current component of the coil current is absorbed through the capacitance.

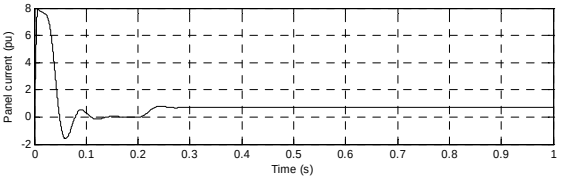

Fig. 8 Panel current

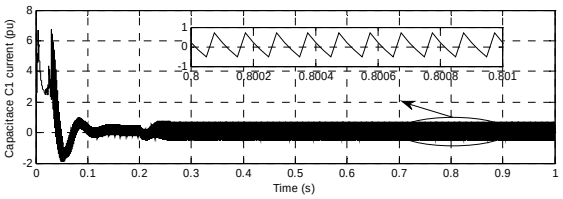

Fig. 9 Capacitance C1 current

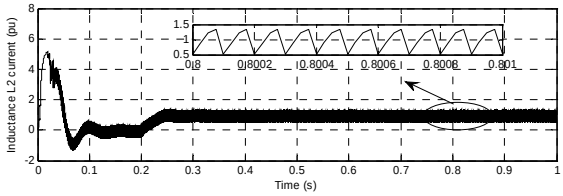

Fig. 10 Inductance L2 current

B. Analyses of physical sizes relating to the PMSM

Initially, the PMSM is at stopped, at $t = 0.2\,s$, a reference direct current equal to zero and a reference quadratic current (fig. 11) was applied to the motor.

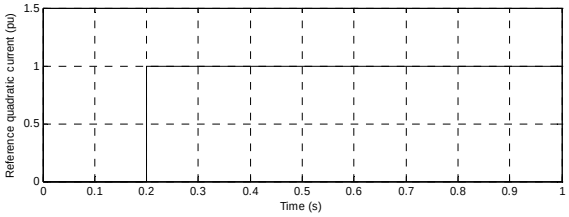

Fig. 11 Reference quadratic current

The response of the direct and the quadratic current are respectively given fig. 12 and fig. 13. It's shown that they converge strictly to their reference.

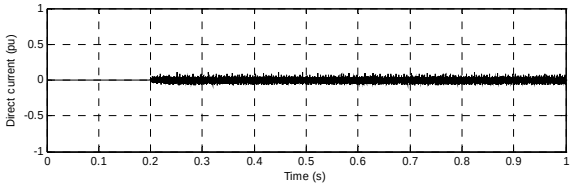

Fig. 12 Direct current response

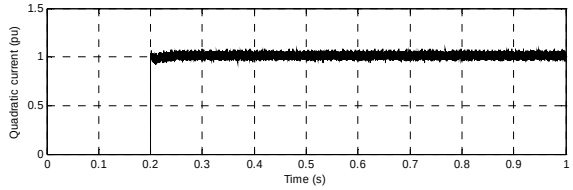

Fig. 13 Quadratic current response

The electromagnetic torque response is given by fig. 14, it converges towards the rated value.

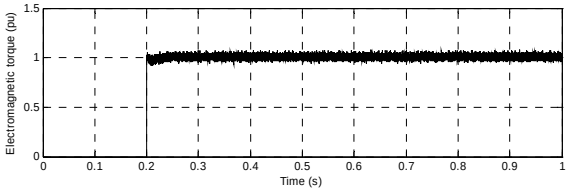

Fig. 14 Electromagnetic torque

V. CONCLUSION

The presented research work leads to the development of an FOC drive scheme for an isolated photovoltaic water pumping system.

Photovoltaic panel supplying a PMSM coupled to a centrifuge pump has been found suitable for remote area application. An inverter is used to adapt the supply conversion an order to perform the FOC PMSM drive.

The buck converter provides a stepped-down voltage to the load when panel voltage stepped-up in order to adapt the required voltage load against insolation variation.

Simulation results are presented highlighting the overall proposed good performances of the system. These promising results open the possibility for the reconstitution of the proposed scheme to be set up for an on-line implementation.

TABLE I. PMSM PARAMETERS

Rated voltage V_s	220 V
Rated current I_N	3.3 A
Rated torque C_{emN}	8.1 N.m
Rated speed Ω_N	210 rad / s
Pole pairs p	4
Rotor flux Φ_r	0.61 Wb
Stator resistance R_s	2.015 Ω
d-axis inductance L_d	22.2 mH
d-axis inductance L_q	22.2 mH

TABLE II. PARAMETERS OF PV CELL (POLLY-CRYSTALLINE SILICON)

Open circuit voltage: V_{oc}	$0.6058\ V$
Short circuit current : I_{sc}	$8.1\ A$
Parallel cell's resistance: R_{pc}	$0.833\ \Omega$
Series cell's resistance: R_{sc}	$0.0833\ m\Omega$
Solar cell's ideal factor : k	1.450
reverse diode saturation current I_{rs}	$3.047e-7\ A$
Short circuit current temperature coefficient K_{SCT}	$1.73e-3A/°K$
Reference cell's temperature: T_{c_ref}	$25°C$
Boltzmann's constant: β	$1.38e-23$
Band gap energy: E_g	$1.11ev$

TABLE III. PARAMETERS OF PV MODULE

Rated output power	$216W$
Open circuit voltage: V_{oc}	$36.35\ V$
Number of series cells: n_s	60

TABLE IV. PV ARRAY PARAMETERS

Open circuit voltage: V_{oc}	$763\ V$
Short circuit current : I_{sc}	$8.1\ A$
Number of series modules: N_s	21
Number of parallel modules: N_p	1

REFERENCES

[1] N. Hidouri, S. Hammadi, L. Sbita, "An Advanced DPC-Self Excited Induction Generator Drive Scheme for an Isolated Wind turbine Boost System," International Review on Modelling and Simulations (IREMOS), vol. 5, No. 2, pp. 913-920, 2012.

[2] Tomás Perpétuo Corrêa, Seleme Isaac Seleme Jr., Selênio Rocha Silva, "Efficiency optimization in stand-alone photovoltaic pumping system", Renewable Energy, Volume 41, pp 220-226, 2012.

[3] N. Hidouri , L. Sbita, "A New DTC-SPMSM Drive Scheme for PV Pumping System, International Journal of Systems Control," vol.1.3, pp. 113-121, 2010.

[4] A.H.M.A Rahim, M. Ahsanul Alam, M.F. Kandlawala, "Dynamic performance improvement of an isolated wind turbine induction generator," Computer and electric Engineering, vol. 35 N 4, pp. 594-607, 2009.

[5] S. Hammadi, N. Hidouri, L. Sbita, "A DTC-DFIG Drive Scheme for an Isolated Wind turbine Buck System," 10th International Multi-Conference on Systems, Signals & Devices SSD-13.

[6] S. Hammadi, N. Hidouri, L. Sbita, "A DTC-Induction-Generator drive scheme for an isolated wind turbine system," 16th IEEE Mediterranean Electrotechnical Conference (MELECON 2012), Medina Yasmine Hammamet Tunisia, (2012).

[7] A. M. Kassem, Modeling, "Analysis and Neural MPPT Control Design of a PV Generator Powered DC Motor-Pump System," WSEAS TRANSACTIONS on SYSTEMS, Issue 12, Volume 10.12, pp. 399-412, 2012.

[8] A. Terki, A. Moussi, A. Betka, N. Terki, "An improved efficiency of fuzzy logic control of PMBLDC for PV pumping system," Applied Mathematical Modelling, Volume 36, No 3, pp. 934–944, 2012.

[9] M. Makhlouf, F. Messai, H. Benalla, "vectored command of induction motor pumping system supplied by photovoltaic generator," Journal of ELECTRICAL ENGINEERING, VOL. 62, NO. 1, pp. 3–10, 2011.

[10] BLASCHKE. F, "The principle of field orientation as applied to the new transvector closed-loop control system for rotating-field machines," Siemens Review, vol. 39, No 5, pp. 217-220, 1972.

[11] S. peresada, A. Tonielli, R. Morici, "High - performance indirect field-oriented output-feedback control of induction motors," Automatica, Vol 35, pp. 1033-1047, 1999.

[12] H. Rehman, A. Dhouadi, "A Fuzzy learning-sliding mode controller for direct field-oriented induction machines," Neurocomputing Vol.71, pp. 2693-2701, 2008.

[13] T. Bjazic, Z. Ban, I. Volaric, "Control of a Fuel Cell Stack loaded with DC/DC Boost Converter," Industrial Electronics. IEEE International Symposium, pp. 1489–1494, 2008.

[14] R. Chenni, M. Makhlouf, T. Kerbache, A. Bouzid, "A detailed modeling method for photovoltaic cells," Energy, vol 32, pp. 1724–1730, 2008.

[15] K.H. Chao, S.H. Ho, M.H. Wang, "Modeling and fault diagnosis of a photovoltaic system," Electric Power Systems Research, vol.78, pp.97–105, 2008.

[16] L.S.Kim, "Sliding mode controller for the single phase grid-connected photovoltaic system," Applied Energy, vol.83, pp. 1101–1115, 2006.

[17] N. Hidouri, T. Mhamdi, S. Hammadi, L. Sbita, "A New hybrid photovoltaic-diesel system control scheme for an isolated load," International Journal of Research and Reviews in Applied Sciences, vol. 9.2, pp. 270-281, 2011.